

Studies on the non-isothermal kinetics of the thermal decomposition of $[\text{Cu}(\text{NBOCTB})](\text{ClO}_4)_2 \cdot 2\text{DMF}$

Li Xiao-Yan ^{a,*}, Sun Hong-Jian ^a, Yang Zhao-He ^b

^a Department of Chemistry, Shandong University, Jinan, Shandong 250100, People's Republic of China

^b Institute of Crystal Materials, Shandong University, Jinan, Shandong 250100, People's Republic of China

Received 28 January 1994; accepted 28 June 1994

Abstract

The thermal decomposition process of the complex $[\text{Cu}(\text{NBOCTB})](\text{ClO}_4)_2 \cdot 2\text{DMF}$ has been studied by the TG–DTG technique, and possible intermediate products of the thermal decomposition are conjectured. The results suggest that the decomposition of the complex can be divided into four steps: $[\text{Cu}(\text{NBOCTB})](\text{ClO}_4)_2 \cdot 2\text{DMF} \xrightarrow{50-198\text{ C}} [\text{Cu}(\text{NBOCTB})](\text{ClO}_4)_2 \cdot \text{DMF} \xrightarrow{198-240\text{ C}} [\text{Cu}(\text{NBOCTB})]\text{ClO}_4 \xrightarrow{240-436\text{ C}} [\text{Cu}(\text{OCTB})]\text{ClO}_4 \xrightarrow{436-610\text{ C}} \text{CuCl}$. The non-isothermal kinetics of steps 1 and 2 have been studied from the TG–DTG curves by means of the Achar et al. and Coats–Redfern methods. Steps 1 and 2 are both three-dimensional diffusion (spherical symmetry) and their kinetic equation can be expressed as $\frac{d\alpha}{dt} = A e^{-E/RT} (3/2)(1-\alpha)^{(2/3)} [1 - (1-\alpha)^{(1/3)}]^{-1}$. The corresponding kinetic compensation effect expressions are found to be $\ln A = 0.2781E - 4.855$ and $\ln A = 0.2403E - 3.758$, respectively.

Keywords: Copper compound; Coupled technique; Kinetics; Macrocyclic complex; Non-isothermal

1. Introduction

There has been recent interest in the study of macrocyclic complexes containing copper atoms as possible models for biochemically important proteins and enzymes

* Corresponding author

[1]. It has been generally accepted that imidazole groups play an important role in the coordination chemistry of the copper ion in many copper-containing proteins [2]. The present paper reports the possible process and mechanism functions of thermal decomposition of the complex of copper(II) with *N,N,N',N'*-tetra-[(1'-benzyl-2'-benzimidazole)methyl]-*trans*-1,2-diaminocyclohexane (NBOCTB), $[\text{Cu}(\text{N4BOCTB})](\text{ClO}_4)_2 \cdot 2\text{DMF}$, together with the corresponding kinetic compensation effect expressions obtained from the non-isothermal TG–DTG curve.

2. Experimental

2.1. Synthesis of NBOCTB · H₂O

In the light of Ref. [3], *ortho*-bis[*N,N'*-bis(2'-benzoimidazolylmethyl)amino]-*trans*-cyclohexane (OCTB) was prepared by condensation of *ortho*-phenylenediamine and 1,2-diamino-cyclohexane-*N,N,N',N'*-tetraacetic acid (CyDTA). OCTB and $\text{BrCH}_2\text{C}_6\text{H}_5$ were stoichiometrically dissolved in a suitable amount of acetone, solid KOH was then added and the solution was warmed for 20 min. To the resulting solution a suitable amount of DMSO was added and stirred continually for 50 min. The solution was cooled and filtered. The solid obtained was washed with water and absolute ethanol several times and dried in a vacuum oven at 40°C. The product was a white powder with m.p. 202–206°C; the yield was 92%. Analytical data for the ligand $\text{C}_{66}\text{H}_{64}\text{N}_{10}\text{O}$ were, found (calcd.)/%: C, 78.32(78.23); H, 5.94(6.37); N, 12.98(13.32). ¹H NMR, δ_{H} , 7.43(8H), 6.85(8H) (16H in benzene ring of benzimidazole); 7.14(20H) (20H in benzene ring of benzyl); 5.36(4H), 5.61(4H) (4CH₂ of benzyl).

2.2. Preparation of the complex $[\text{Cu}(\text{NBOCTB})](\text{ClO}_4)_2 \cdot 2\text{DMF}$

To a DMF solution (50 cm³) of NBOCTB (0.25 mmol) was added an ethanol solution (10 cm³) of $\text{Cu}(\text{ClO}_4)_2$ (2 mmol) with constant stirring under reflux for about 5 min. The resulting green solution was evaporated at room temperature in air for about a week to give green crystals of the complex $[\text{Cu}(\text{NBOCTB})](\text{ClO}_4)_2 \cdot 2\text{DMF}$. Elementary analyses and single-crystal X-ray diffractational analysis showed that its molecular formation conformed to $[\text{Cu}(\text{NBOCTB})](\text{ClO}_4)_2 \cdot 2\text{DMF}$.

2.3. Apparatus and measurements

Copper was determined using a USA 8451A UV–vis spectrophotometer. Carbon, hydrogen and nitrogen analyses were carried out on a Perkin-Elmer 240C elemental analyser. Chlorine was determined gravimetrically [4]. ¹H NMR spectra were recorded on a FX-90Q NMR Spectrometer (Japan). Melting points were measured on a Model X₄ melting point meter (Shanghai, People's Republic of China).

The TG–DTG curve was obtained using a Perkin-Elmer model TGS-2 thermo-balance. The heating rate was $5^{\circ}\text{C min}^{-1}$ and the flow rate of N_2 gas was $40 \text{ cm}^3 \text{ min}^{-1}$. The experiment was performed between 40°C and 750°C .

3. Results and discussion

3.1. Thermal decomposition process

The TG and DTG curves of $[\text{Cu}(\text{NBOCTB})](\text{ClO}_4)_2 \cdot 2\text{DMF}$ are shown in Fig. 1.

Through the combination of TG and DTG curves and elemental analyses of the intermediate products we have deduced that the probable thermal decomposition steps of $[\text{Cu}(\text{NBOCTB})](\text{ClO}_4)_2 \cdot 2\text{DMF}$ are as shown in Table 1. The elemental analyses of the intermediate are listed in Table 2 and are in agreement with the given formulae.

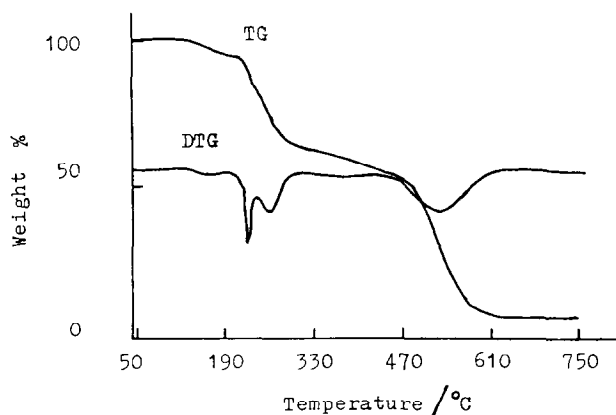


Fig. 1. The TG and DTG curves of $[\text{Cu}(\text{NBOCTB})](\text{ClO}_4)_2 \cdot 2\text{DMF}$.

Table 1
Thermal decomposition process of $[\text{Cu}(\text{NBOCTB})](\text{ClO}_4)_2 \cdot 2\text{DMF}$

Step	Decomposition process	Mass loss/% ^a
1	$[\text{Cu}(\text{NBOCTB})](\text{ClO}_4)_2 \cdot 2\text{DMF} \xrightarrow{50-198\text{ C}} [\text{Cu}(\text{NBOCTB})](\text{ClO}_4)_2 \cdot \text{DMF}$ (I)	5.24 (5.20)
2	$[\text{Cu}(\text{NBOCTB})](\text{ClO}_4)_2 \cdot \text{DMF} \xrightarrow{198-240\text{ C}} [\text{Cu}(\text{NBOCTB})]\text{ClO}_4$ (II)	12.50 (12.29)
3	$[\text{Cu}(\text{NBOCTB})]\text{ClO}_4 \xrightarrow{240-436\text{ C}} [\text{Cu}(\text{OCTB})]\text{ClO}_4$ (III)	25.70 (25.64)
4	$[\text{Cu}(\text{OCTB})]\text{ClO}_4 \xrightarrow{436-610\text{ C}} \text{CuCl}$	48.72 (49.82)

^a Values in parentheses are calculated values.

Table 2
Elemental analyses (in %) of the intermediate products

Intermediate products		Cu	C	H	N	Cl
(I)	Calc.	4.78	62.28	5.19	11.58	5.34
	Found	5.05	61.70	4.93	11.68	5.00
(II)	Calc.	5.49	68.45	5.36	12.10	3.07
	Found	5.30	69.01	5.50	11.90	3.16
(III)	Calc.	7.96	57.21	4.80	17.56	4.44
	Found	7.56	57.73	5.06	17.98	4.22

3.2. Non-isothermal kinetics for Steps 1 and 2

For the TG and DTG curves (Fig. 1), we use the equations of Achar et al. [5] and Coats and Redfern [6] to analyse Steps 1 and 2.

Archarr equation

$$\ln[(d\alpha/dt)/f(\alpha)] = \ln A - E/(RT) \quad (1)$$

Coats–Redfern equation

$$\ln[g(\alpha)/T^2] = \ln(AR)/(\beta E) - E/(RT) \quad (2)$$

In the above equations, α is the fraction of the reacted material, T is the absolute temperature and $f(\alpha)$ and $g(\alpha)$ are differential and integral mechanism functions, respectively. E and A are the derived apparent activation energy and pre-exponential factor, respectively, R is the gas constant and β is the heating rate.

Table 3
Kinetic functions used for the analysis

Function no.	Differential form $f(\alpha)$	Integral form $g(\alpha)$
1	$1/2\alpha$	α^2
2	$[-\ln(1-\alpha)]^{-1}$	$\alpha + (1-\alpha) \ln(1-\alpha)$
3	$3[(1-\alpha)^{-1/2}-1]^{-1/2}$	$(1-2\alpha/3) - (1-\alpha)^{2/3}$
4	$3(1-\alpha)^{2/3}[1-(1-\alpha)^{1/3}]^{-1/2}$	$[1-(1-\alpha)^{1/3}]^2$
5	$(1-\alpha)$	$-\ln(1-\alpha)$
6	$3(1-\alpha)[- \ln(1-\alpha)]^{1/3}/2$	$[- \ln(1-\alpha)]^{1/1.5}$
7	$2(1-\alpha)[- \ln(1-\alpha)]^{1/2}$	$[- \ln(1-\alpha)]^{1/2}$
8	$3(1-\alpha)[- \ln(1-\alpha)]^{2/3}$	$[- \ln(1-\alpha)]^{1/3}$
9	$4(1-\alpha)[- \ln(1-\alpha)]^{3/4}$	$[- \ln(1-\alpha)]^{1/4}$
10	$2(1-\alpha)^{1/2}$	$1-(1-\alpha)^{1/2}$
11	$3(1-\alpha)^{2/3}$	$1-(1-\alpha)^{1/3}$
12	1	α
13	$2\alpha^{1/2}$	$\alpha^{1/2}$
14	$(1-\alpha)^2$	$(1-\alpha)^{-1}-1$
15	$2(1-\alpha)^{3/2}$	$(1-\alpha)^{-1/2}$

Table 4
Data for Step 1 of decomposition of $[\text{Cu}(\text{NBOCTB})](\text{ClO}_4)_2 \cdot 2\text{DMF}$ obtained from the TG and DTG curves

No.	T_i/K	α_i	$(d\alpha/dt)_i/\text{min}^{-1}$
1	398.15	0.1423	0.6400
2	405.15	0.2327	0.9600
3	411.15	0.2492	1.0933
4	417.15	0.3673	1.2267
5	423.15	0.4250	1.8000
6	429.15	0.5327	2.8667
7	431.15	0.5962	3.3333
8	433.15	0.6558	3.1333
9	437.15	0.7250	1.6400
10	445.15	0.7942	0.6267

The possible forms of $f(\alpha)$ and $g(\alpha)$ are listed in Table 3. The original data for Steps 1 and 2 determined from the TG–DTG curves are listed in Tables 4 and 5, respectively.

Using the possible forms of $f(\alpha)$ and $g(\alpha)$ in Table 3, the data in Tables 4 and 5 have been analysed by use of Eqs. (1) and (2). For Eqs. (1) and (2) the kinetic analyses were completed by the linear least-squares method on a TI-59 computer. The results are shown in Tables 6 and 7, respectively.

The results in Tables 6 and 7 clearly show that the values E and A obtained from the two equations are approximately the same and the linear correlation coefficients are better when the probable mechanism function is logically function no. 4 (in Table 3). We concluded that Steps 1 and 2 are both three-dimensional diffusion (spherical symmetry). The non-isothermal kinetic equation for Steps 1 and 2 is

$$d\alpha/dt = Ae^{-E/RT} \left(\frac{3}{2}\right) (1-\alpha)^{(2/3)} [1 - (1-\alpha)^{(1/3)}]^{-1}$$

Table 5
Data for Step 2 of decomposition of $[\text{Cu}(\text{NBOCTB})](\text{ClO}_4)_2 \cdot 2\text{DMF}$ obtained from the TG and DTG curves

No.	T_i/K	α_i	$(d\alpha/dt)_i/\text{min}^{-1}$
1	485.15	0.0848	1.5278
2	489.15	0.1472	2.1528
3	492.15	0.1888	3.3056
4	494.15	0.2392	4.8611
5	496.15	0.3216	7.9167
6	498.15	0.4480	9.7639
7	499.15	0.5280	9.4167
8	500.15	0.5944	8.4306
9	501.15	0.6592	6.8750
10	503.15	0.7360	4.6528

Table 6
Results of analysis of the data for Step 1 in Table 4 using the equations of Achar et al. [5] (Eq. (1)) and Coats and Redfern [6] (Eq. (2))

No.	Coats–Redfern method			Achar method		
	$E/(\text{kJ mol}^{-1})$	$\ln(A/\text{s}^{-1})$	r	$E/(\text{kJ mol}^{-1})$	$\ln(A/\text{s}^{-1})$	r
1	100.52	21.71	0.9869	79.98	18.88	0.7961
2	111.57	24.46	0.9906	99.10	23.98	0.8656
3	115.90	24.32	0.9918	106.75	24.76	0.8867
4	124.71	27.08	0.9934	121.38	29.18	0.9169
5	65.93	12.63	0.9939	70.17	16.98	0.8342
6	41.60	5.43	0.9932	45.81	9.84	0.7090
7	29.43	1.72	0.9924	33.67	6.19	0.5972
8	17.29	−2.18	0.9901	21.53	2.41	0.4323
9	11.22	−4.31	0.9868	15.46	0.44	0.3264
10	55.62	8.67	0.9912	48.14	9.68	0.6908
11	58.86	9.31	0.9925	55.54	11.48	0.7497
12	46.77	12.50	0.9848	26.19	3.74	0.4294
13	19.71	−1.63	0.9796	−0.66	−4.02	0.0126
14	90.71	20.41	0.9912	114.07	30.22	0.9414
15	14.97	−2.45	0.9042	93.78	23.42	0.9012

3.3. The kinetic compensation effect

According to the mathematical expression for the kinetic compensation effect ($\ln A = aE + b$, Ref. [7]) we fitted the kinetic parameters obtained (E and A) using

Table 7
Results of analysis of the data for Step 2 in Table 5 using the equations of Achar et al. [5] (Eq. (1)) and Coats and Redfern [6] (Eq. (2))

No.	Coats–Redfern method			Achar method		
	$E/(\text{kJ mol}^{-1})$	$\ln(A/\text{s}^{-1})$	r	$E/(\text{kJ mol}^{-1})$	$\ln(A/\text{s}^{-1})$	r
1	504.16	116.16	0.9954	445.55	105.16	0.9554
2	541.24	124.71	0.9949	507.74	119.84	0.9726
3	555.46	126.72	0.9945	531.60	124.22	0.9773
4	583.98	133.84	0.9937	577.74	135.61	0.9837
5	310.20	70.02	0.9917	327.82	77.62	0.9659
6	204.02	44.14	0.9915	221.65	51.76	0.9289
7	150.98	31.10	0.9912	168.60	38.74	0.8836
8	97.94	17.95	0.9908	115.56	25.60	0.7861
9	71.42	11.26	0.9903	88.96	18.96	0.6963
10	277.36	61.11	0.9942	258.56	58.84	0.9250
11	287.91	63.34	0.9935	281.68	65.14	0.9430
12	248.01	54.44	0.9952	189.31	43.46	0.8255
13	119.89	23.20	0.9949	61.23	12.24	0.4345
14	386.52	89.06	0.9832	449.79	107.90	0.9829
15	61.02	9.10	0.8916	397.08	94.01	0.9812

Table 8
Kinetic compensation parameters for $[\text{Cu}(\text{NBOCTB})](\text{ClO}_4)_2 \cdot 2\text{DMF}$

Step	<i>a</i>	<i>b</i>	<i>r</i>
1	0.2781	−4.8548	0.9835
2	0.2403	−3.7582	0.9990

the equations of Achar et al. and Coats and Redfern (see Tables 6 and 7) by the linear least-squares method on a TI-59 computer, and obtained the kinetic compensation parameters *a* and *b*. The results indicate that the kinetic parameters *E* and *A* may be connected through *a* and *b*. The values of *a* and *b* for Steps 1 and 2 are given in Table 8.

Acknowledgement

This project was supported by the National Natural Science Youth Foundation of China.

References

- [1] N. Sorrell, *Tetrahedron*, 45 (1989) 3.
- [2] R.D. Bereman and D.J. Kosman, *J. Am. Chem. Soc.*, 99 (1977) 7322.
- [3] H.M.J. Hendriks, P.J.M.W.L. Birker, J. van Rijn, G.C. Verschoor and J. Reedijk, *J. Am. Chem. Soc.*, 104 (1982) 3607.
- [4] A.I. Vogel, *Vogel's Textbook of Quantitative Inorganic Analysis*, 4th edn., Longman, London, 1978, p. 434.
- [5] B.N. Narahari Achar, G.W. Bridley and J.H. Sharp, *Proc. Int. Clay Conf.*, Jerusalem, 1966, Vol. 1, p. 67.
- [6] A.W. Coats and J.P. Redfern, *Nature*, 201 (1964) 68.
- [7] J. Zsako, *J. Thermal Anal.*, 9 (1976) 101.